

# MSBOTS: a Multiple Small Biological Organism Tracking System robust against non-Ideal detection and segmentation conditions

Xiaoying Wang<sup>Corresp., 1</sup>, Eva Cheng<sup>2</sup>, Ian S Burnett<sup>2</sup>

<sup>1</sup> School of Engineering, RMIT University, Melbourne, Australia

<sup>2</sup> Faculty of Engineering & Information Technology, University of Technology Sydney, Sydney, New South Wales, Australia

Corresponding Author: Xiaoying Wang  
Email address: xiaoying.wang@rmit.edu.au

Accurately tracking a group of small biological organisms using algorithms to obtain their movement trajectories is essential to biomedical and pharmaceutical research. However, object mis-detection, segmentation errors and overlapped individual trajectories are particularly common issues that restrict the development of automatic multiple small organism tracking research. Extending on previous work, this paper presents an accurate and generalised Multiple Small Biological Organism Tracking System (MSBOTS), whose general feasibility is tested on three types of organisms. Evaluated on zebrafish, Artemia and Daphnia video datasets with a wide variety of imaging conditions, the proposed system exhibited decreased overall Multiple Object Tracking Precision (MOTP) errors of up to 77.59%. Moreover, MSBOTS obtained more reliable tracking trajectories with a decreased standard deviation of up to 47.68 pixels compared with the state-of-the-art idTracker system. This paper also presents a behaviour analysis module to study the locomotive characteristics of individual organisms from the obtained tracking trajectories. The developed MSBOTS with the locomotive analysis module and the tested video datasets are made freely available online for public research use.

# MSBOTS: a Multiple Small Biological Organism Tracking System robust against non-ideal detection and segmentation conditions

Xiaoying Wang<sup>1</sup>, Eva Cheng<sup>2</sup>, and Ian S. Burnett<sup>2</sup>

<sup>1</sup>RMIT University, School of Engineering, Melbourne, 3000, Australia

<sup>2</sup>University of Technology Sydney, Faculty of Engineering & Information Technology, Sydney, 2007, Australia

Corresponding author:

Xiaoying Wang<sup>1</sup>

Email address: xiaoying.wang@rmit.edu.au

## ABSTRACT

Accurately tracking a group of small biological organisms using algorithms to obtain their movement trajectories is essential to biomedical and pharmaceutical research. However, object mis-detection, segmentation errors and overlapped individual trajectories are particularly common issues that restrict the development of automatic multiple small organism tracking research. Extending on previous work, this paper presents an accurate and generalised Multiple Small Biological Organism Tracking System (MSBOTS), whose general feasibility is tested on three types of organisms. Evaluated on zebrafish, *Artemia* and *Daphnia* video datasets with a wide variety of imaging conditions, the proposed system exhibited decreased overall Multiple Object Tracking Precision (MOTP) errors of up to 77.59%. Moreover, MSBOTS obtained more reliable tracking trajectories with a decreased standard deviation of up to 47.68 pixels compared with the state-of-the-art idTracker system. This paper also presents a behaviour analysis module to study the locomotive characteristics of individual organisms from the obtained tracking trajectories. The developed MSBOTS with the locomotive analysis module and the tested video datasets are made freely available online for public research use.

## INTRODUCTION

In recent years, small biological organisms such as zebrafish larvae (genetically and physiologically similar to humans), *Artemia franciscana*, and *Daphnia magna* have become powerful models and are widely used to study human disease (James et al., 2019), pharmacology (Comeche et al., 2017) and ecotoxicology (James et al., 2019; Comeche et al., 2017; Poynton et al., 2007). Accurate tracking techniques are vital for understanding the biology and ecology underlying their movement (Martineau and Mourrain, 2013; Nema et al., 2016; Colwill and Creton, 2011; Alyuruk et al., 2013; Ekvall et al., 2013). The traditional method relying on human visual observations is very tedious and time consuming. Also, the related experiments are difficult to reliably repeat. Though fluorescent labelling can improve the visual distinction of specific targets, fluorescent materials affect the behavioural response of these organisms (Ekvall et al., 2013).

Automatic object tracking techniques have assisted in developing approaches to the behaviour analysis of large organisms such as mammals, birds and adult fish. However, the tracking of small organisms are hampered by the constraints of existing automatic tracking systems (Ekvall et al., 2013; Dur et al., 2011) as most organisms are considerably smaller than 1 mm (Marechal et al., 2004). There are many challenges imposed by the small sized organisms. Firstly, the widely used transponder (also called u-chips) in individual organism identification dramatically affect the natural behaviour of organisms within millimetre-scales (Ekvall et al., 2013; Lard et al., 2010) when affixing to their bodies, because the currently available smallest chip size is around 0.4 mm (Usami, 2004; Rashid et al., 2012). In addition, general object tracking is already a complex problem due to object occlusion, non-rigid structure

45 (caused by object rotation and scale changes), and motion pattern changes (Habibi et al., 2017). The  
46 challenge increases when the tracking targets are small in size, because small organisms provide very  
47 little information compared with imaging noise.

48 Existing automatic tracking systems for multiple organisms (Zhou et al., 2014; Conklin et al., 2015)  
49 either use adult subjects (Pérez-Escudero et al., 2014) in a large container to limit object interaction, or  
50 use a petri dish plate to separate individual objects, allowing only one object in each dish well to avoid  
51 overlapped and swapped trajectories. The machine learning based CNNTracker (Zhiping and Cheng,  
52 2017) attempts to optimise individual identification accuracy by creating zebrafish head feature maps.  
53 However, this system only tested on adult zebrafish, which have very different movement characteristics  
54 and higher target-background imaging contrast than small sized larval organisms. Thus, this method may  
55 mis-classify larval organisms with multiple identities (Zhiping and Cheng, 2017). The Generalized Linear  
56 Mixed Model (GLMM) (Liu et al., 2017) studies the analysis of larval locomotive activities, but can only  
57 detect whether movement exists by reporting binary move/no-move classes, but does not enable object  
58 displacement estimation.

59 Accurate object detection and segmentation provides a critical foundation for the performance of the  
60 subsequent tracking process. However, the results of existing Multiple Target Tracking (MTT) algorithms  
61 degenerate caused by false positive segmentation (i.e., noise fragments remaining after segmentation)  
62 and false negative segmentation (i.e. mis-detected objects and occluded objects) (Mallick et al., 2013).  
63 Such segmentation challenges commonly occur in microscopic small organism videos when taken under  
64 realistic experimental conditions (without deliberate imaging control). It is nearly impossible to identify  
65 and segment all small organisms without picking up noise using these microscopic videos (Noss et al.,  
66 2013). Non-ideal tracking results further pose challenges for behavioural analysis and maintaining  
67 individual identities over time (Martineau and Mourrain, 2013).

68 IdTracker (Pérez-Escudero et al., 2014) is a well-known biological organism tracking system with  
69 ‘fingerprint’ generation for subject identity differentiation, and the commercial LoliTrack (Závorka et al.,  
70 2017) system can also track multiple targets in a single container. However, both systems require the  
71 input videos to be taken under strict imaging conditions. As reported by Zhou et al. (2014) and Noss  
72 et al. (2013), even small impurities inside water (e.g., water bubbles) or lighting reflections (e.g., surface  
73 ripples) affect the object segmentation accuracy.

74 3D systems with multiple cameras or super-resolution images built from multiple low-resolution  
75 images are presented to obtain more information for accurate tracking of small organisms (Ekvall et al.,  
76 2013; Günel et al., 2019; Noss et al., 2013). However, these systems increase computational complexity,  
77 change data association structure, and require further location registration among cameras or images. Thus,  
78 these challenges constrain the real-time application of these techniques in tracking multiple small-scaled  
79 organisms (Günel et al., 2019).

80 Extending on our previous work (Wang et al., 2017a, 2018), this paper presents an automatic and  
81 accurate Multiple Small Biological Organism Tracking System (MSBOTS). The approach is robust against  
82 non-ideal object detection and segmentation results that are obtained from microscopic time-lapse videos  
83 taken under practical laboratory experimental conditions. The system applies Gaussian Mixture Model  
84 (GMM) based background subtraction in the segmentation module (Wang et al., 2017a) to detect and  
85 segment small organisms from each video frame, and initially maps detected objects between successive  
86 video frames based on the (non-ideal) segmentation results using the Hungarian algorithm (also called  
87 Kuhn–Munkres algorithm) (Bourgeois and Lassalle, 1971; Munkres, 1957). The positions of mis-detected  
88 and overlapped objects are then calculated through their neighbour’s locations. Then the theoretically  
89 computed locations are bridged in the individual tracking trajectories (Wang et al., 2018). This paper  
90 extends on this existing work to present a novel behaviour analysis module to implement locomotive  
91 behaviour analysis such as estimating object velocities, accelerations and movement directions. The  
92 performance and versatility of MSBOTS is then evaluated and demonstrated by tracking accuracy, and  
93 compared with existing multiple organism tracking systems using a zebrafish larvae video dataset (Wang  
94 et al., 2017a) as used in our previous work. In this paper, to evaluate the generalisation of the proposed  
95 system to track other small-sized organisms, we also apply the system to video datasets of another two  
96 types of small organisms *Artemia franciscana*, and *Daphnia magna*).

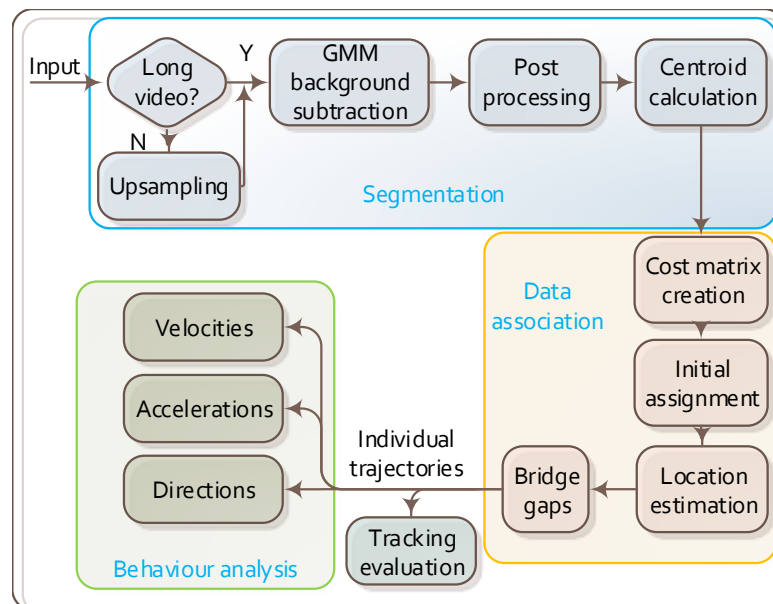


**Figure 1.** Flow chart of the proposed MSBOTS platform. It takes microscopic time-lapse frames as input, and consists of three main modules: object segmentation, data association based on the centroid locations of detected objects, and the behaviour analysis using the obtained individual trajectories.

## 97 METHODS

98 Fig. 1 outlines the overall workflow of the proposed MSBOTS platform, which comprises an object  
 99 segmentation module(Wang et al., 2017a), data association module (Wang et al., 2018) and the behaviour  
 100 analysis module novel to this paper. The accurate differentiation of organisms from the image background  
 101 and foreign matter (such as water impurities and objects faeces) in each video frame is the critical  
 102 foundation for this system. Here, the image background is estimated by an adaptive Gaussian Mixture  
 103 Model (GMM) (Zivkovic and Heijden, 2006) in the segmentation module. Organisms in every video  
 104 frame are segmented after the background subtraction; details of this segmentation approach can be found  
 105 in our previous work (Wang et al., 2017a). The following data association module assigns detected objects  
 106 (as sources, represented by the computed centroids of segmented regions) to their corresponding targets in  
 107 the successive frames. This part plays an essential role in maintaining consistent individual identities for  
 108 the detected organisms over time; details of this approach are in Wang et al. (2018). The data association  
 109 (also called mapping) algorithm not only finds the most likely targets in the following frames for detected  
 110 organisms, but also calculates the theoretical positions for mis-detected or occluded organisms. After  
 111 obtaining the individual trajectories of all organisms from the output of the data association module, the  
 112 movement characteristics of each organism are then estimated in the novel behaviour analysis module  
 113 proposed in this paper as shown in Fig. 1.

114 This platform as a whole (as shown in Fig. 1) is tested on a zebrafish video dataset as used in our  
 115 previous work (Wang et al., 2017a, 2018), and another two new video datasets of two different types of  
 116 small organisms to evaluate the generalisation of our approach.

## 117 Code of ethics

118 Ethics approval is not required when filming videos of larval organisms. Further, no chemicals were tested  
 119 with the larval organisms being filmed. The adult zebrafish video analysed is from a publicly available  
 120 online repository (Pérez-Escudero et al., 2014).

## 121 Organism detection and segmentation

122 In the background subtraction step of the proposed MSBOTS platform, an improved GMM (Zivkovic and  
 123 Heijden, 2006) was chosen to estimate the stationary background due to its ability to extend the detection  
 124 period (Wang et al., 2017a). This is particularly effective for addressing the imbalanced movement  
 125 problem of small biological organisms that occur in time-lapse microscopic video frames. As reported by

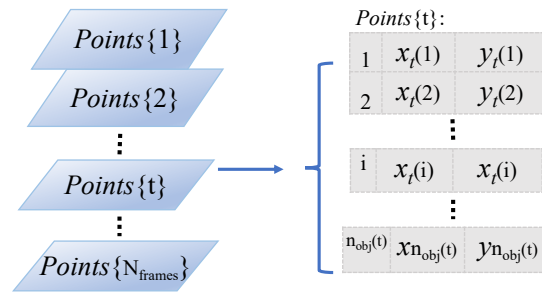


**Figure 2.** Storage structure of detected objects in a video sequence. The light blue parallelogram series represent the detected organisms within each time-lapse frame. And the cell array  $Points\{t\}$  on the right side shows the detailed data storage structure (that is how the individual identities and object Euclidean locations are arranged) of the detected objects in the example frame  $t$ .

126 Liu et al. (2017), small organisms such as zebrafish larvae exhibit a mean proportion of activities less than  
 127 7.5% over time with a 'bursty' movement pattern of sudden swimming motion interspersed with mainly  
 128 stationary periods.

129 After video background estimation, the moving objects can be initially classified as the foreground  
 130 organisms. Due to the 'bursty' movement pattern of small organisms, a moving organism will be firstly  
 131 represented by a new region cluster with a small weight, whose value will be gradually increasing if the  
 132 region remains stationary over time. This new region will not be classified as the background until its  
 133 weight value exceeds a threshold  $c_f$ , which is calculated as in Zivkovic and Heijden (2006). Thus, the  
 134 detection period of a stationary organism can be extended for approximately  $\log(1 - c_f) \setminus \log(1 - \alpha)$   
 135 frames, where  $\alpha$  denotes the constant factor shaping an exponential decay envelope introduced in the  
 136 GMM work by Zivkovic and Heijden (2006). This enables the detection and tracking of organisms that  
 137 stop at a position for a certain period of time before restarting their motion.

138 Furthermore, to adapt to background changes in microscopic videos over time, the adaptive GMM  
 139 (Zivkovic and Heijden, 2006) adds flexibility when selecting the number of Gaussian components and  
 140 their parameters. The approach by Zivkovic and Van Der Heijden (2004) and the Dirichlet criteria  
 141 are applied, respectively, in model initialisation and selection of the number of Gaussian components.  
 142 The Gaussian component parameters are then adaptively updated for each video frame to accurately  
 143 represent background pixels, in contrast to traditional GMM models that apply one or a fixed number  
 144 of components. The foreground objects are then obtained by the differentiation of the video frames  
 145 from the corresponding estimated background. Furthermore, post-processes such as median filtering,  
 146 morphological grayscale erosion, and size-based noise removal are applied to eliminate image distortion  
 147 and scattered noise fragments from the foreground. Within these, the morphological grayscale erosion  
 148 deploys a flat diamond-shaped structuring element to erode the obtained organism foreground image.  
 149 Thus, the boundaries among organisms in very close proximity are further widened; thus, the estimated  
 150 centroid positions of the detected regions are more accurate.

151 The detection and segmentation of MSBOTS enables the removal of stationary backgrounds (such  
 152 as the organism container and labels/markers drawn on its surface) and is robust against unbalanced  
 153 organism movement patterns (e.g., 'bursty' movement) and water impurities. Hence, unlike existing  
 154 systems, MSBOTS is able to process videos under practical experimental imaging conditions.

## 155 Representing detected organisms

156 To represent the positions of the detected organisms in each video frame, the centroid locations of  
 157 segmented foreground regions in Cartesian coordinates are used and stored in a vertical cell array matrix,  
 158 as shown by the parallelogram series (indicating video frames) and  $Points\{t\}$  matrix in Fig. 2. In the  
 159  $Points\{t\}$  cell array, the first column stores the temporary identity, numbered from 1 to the number  
 160 of detected organisms in each video frame, where  $n_{obj}(t)$  indicates the number of detected organisms  
 161 in frame  $t$ . The second and third column stores the horizontal and vertical positions of each detected  
 162 organism in  $x$  and  $y$  coordinates, respectively. This cell array matrix representation allows for varying  
 163 element length (indicating the number of detected organisms in frame  $t$ ), which can change frame-to-frame

164 due to detection and segmentation errors.

### 165 **Organism assignment between frames**

166 The centroid locations of detected organisms are obtained in the segmentation module and represented  
167 frame-by-frame using a cell array for each video sequence as described in the previous section. However,  
168 the organism identities over video frames are still unknown. That is, which organism in the current  
169 frame corresponds to which organism in the following frame has not been mapped. In addition, there  
170 are still some remaining mis-detected organisms that have been classified into background regions or  
171 overlapped with other detected organisms. The data association module of MSBOTS thus builds tracking  
172 trajectories of individual organisms by mapping the detected organisms between successive pairs of  
173 frames, calculating the positions of mis-detected or occluded organisms, and bridging the theoretical  
174 locations back to their correct trajectories by adjusting the initial assignment results.

#### 175 **Initial assignment**

176 The initial frame-by-frame data association of detected organisms is a partial assignment using an  
177 extension of the Kuhn-Munkres algorithm (Bourgeois and Lassalle, 1971) to process the rectangular cell  
178 array  $Points\{t\}$ . Extending on the original Hungarian algorithm (Harold, 1955) that solves the assignment  
179 problem with an equal number of workers and tasks represented by a  $n \times n$  matrix, the number of workers  
180 and tasks can be unequal and represented in a rectangular matrix (Bourgeois and Lassalle, 1971). This  
181 extended algorithm can then be applied to multiple organism tracking, where the number of detected  
182 organisms can change due to non-ideal segmentation resulting from organism mis-detection and occlusion.

183 In the initial assignment process, all the detected organisms annotated by  $Points\{t\}$  in frame  $t$  are  
184 taken as source points, and the segmented organisms  $Points\{t+1\}$  in the following frame  $t+1$  are seen  
185 as the target points. The target points  $Points\{t+1\}$  need to be mapped to the source points  $Points\{t\}$   
186 frame-by-frame across a video sequence. The Euclidean distance of a source point  $S_i$  to a target point  $T_j$   
187 calculated by Equation (1) is the cost to connect this point pair. A matrix  $\mathbb{D}$ , as shown in Equation (2), is  
188 created to represent the cost of assigning source organisms  $S = \{S_1, S_2, S_3, \dots, S_n\}$  in the frame  $t$  to the  
189 target organisms  $T = \{T_1, T_2, T_3, \dots, T_m\}$  in the frame  $t+1$ .

$$190 \quad d_{S_i, T_j} = \sqrt{(x_j - x_i)^2 + (y_j - y_i)^2} \quad (1)$$

$$191 \quad \mathbb{D}(S, T) = \begin{pmatrix} d_{S_1, T_1} & d_{S_1, T_2} & d_{S_1, T_3} & \cdots & d_{S_1, T_m} \\ d_{S_2, T_1} & d_{S_2, T_2} & d_{S_2, T_3} & \cdots & d_{S_2, T_m} \\ \vdots & \vdots & \ddots & \vdots & \vdots \\ d_{S_n, T_1} & d_{S_n, T_2} & d_{S_n, T_3} & \cdots & d_{S_n, T_m} \end{pmatrix} \quad (2)$$

190 where  $n$  and  $m$  are the detected number of organisms in the frame  $t$  and the successive frame  $t+1$ ,  
191 respectively.

192 The frame-to-frame objects mapping searches for unique assignments in the cost matrix  $\mathbb{D}(S, T)$  by  
193 connecting the source organism  $S_i$  in the frame  $t$  to only one target organism  $T_j$  in the successive frame  
194  $t+1$ . The sum of the resultant complete assignments between  $Points\{t+1\}$  and  $Points\{t\}$  is the global  
195 optimum with the lowest overall cost amongst all the possible assignments within two successive frames.  
196 Thus, the assignment seeks for the most likely correspondences for all detected source points in the  
197 successive frame (combinatorial optimisation). The matched target points propagate the identities of  
198 the source points. Thus, connecting the points with the same identities across video frames gives the  
199 individual organism tracking trajectories after calculating the assignment maps for all the successive video  
200 frames.

201 It is possible to avoid the propagation of false positive detections within the segmentation results  
202 when constructing the individual trajectories. In the initial frame-to-frame assignment step, a distance  
203 threshold is set as a constraint in the source-target cost matrix  $\mathbb{D}(S, T)$ . The threshold value is calculated  
204 by  $\delta * \text{median}(d_{S_i, T_j})$ , as in Zhiping and Cheng (2017). When the minimum value of the  $i$ -th row in  
205 the source-target cost matrix  $\mathbb{D}(S, T)$  is larger than the estimated threshold value, this indicates that the  
206 distances between the source point  $S_i$  to all of the points in the successive frame exceed the threshold value.



$$x_{miss} = x_s + \frac{1}{j} * (x_t - x_s) \quad (4)$$

$$y_{miss} = y_s + \frac{1}{j} * (y_t - y_s) \quad (5)$$

250 where  $j$  indicates the following  $j$ -th frame from the unmatched source point.

### 251 **Bridging trajectory gaps for mis-detected and occluded organisms**

252 Individual tracking trajectories for each organism are obtained through connecting the matched points with  
 253 the same identities frame-by-frame over a video sequence. However, the tracking trajectories obtained  
 254 from the initial assignment process are usually trajectory fragments, separated when organisms are mis-  
 255 detected or overlapped, caused by segmentation errors. In the proposed MSBOTS, these trajectory gaps  
 256 are bridged by adding the estimated points of these mis-detected or overlapped organisms as described in  
 257 the previous section.

258 To connect trajectory fragments, the points stored in the unmatched source matrix are mapped to  
 259 the points in the unmatched target matrix, and the positions of the missed points between the newly  
 260 matched unmatched-source to unmatched-target pairs are also calculated during this mapping process.  
 261 For example, as shown in Fig. 3, the unmatched source  $P_i(t)$  as the end point of its trajectory fragment is  
 262 connected to the unmatched target point  $P_i(t+2)$ , which is the start point of its trajectory fragment, and  
 263 the middle point shown by the orange dot is added between points  $P_i(t)$  and  $P_i(t+2)$  as the theoretical  
 264 position of the overlapped point  $P_i(t+1)$ .

### 265 **Locomotion characteristic analysis**

266 After obtaining the individual tracking trajectories for each organism in the video sequence, the movement  
 267 characteristics of these organisms can be analysed. The calculation of three movement parameters,  
 268 movement velocity, acceleration and direction as represented by Equations (6-8), respectively, are  
 269 implemented and presented in this work.

$$velocity = \frac{\sqrt{(x_{t+1}(i) - x_t(i))^2 + (y_{t+1}(i) - y_t(i))^2}}{dt} \quad (6)$$

$$acceleration = \frac{d(velocity)}{d^2t} \quad (7)$$

$$direction = \text{atan2} \frac{y_{t+1}(i) - y_t(i)}{x_{t+1}(i) - x_t(i)} \quad (8)$$

270 where  $dt = 1/fs$  and  $fs$  is the video frame rate, and  $x_t(i)$  and  $y_t(i)$  are the Cartesian coordinates of  
 271 organism  $i$  ( $i$  is the assigned organism identity) in frame  $t$ .

## 272 **RESULTS AND DISCUSSION**

273 To evaluate the performance of MSBOTS, microscopic videos of three types of small biological organisms  
 274 (zebrafish, *Artemia* and *Daphnia*) were tested, where preliminary evaluation using zebrafish was presented  
 275 in our previous work (Wang et al., 2018; Wang, 2018). Evaluated on a set of single and multiple larvae  
 276 and adult zebrafish, *Artemia* and *Daphnia* videos here, a wide variety of (complex) imaging conditions  
 277 were tested, including shadowing, labels (manually drawn on the petri dish), and background artefacts  
 278 (such as water impurities, object faeces and water bubbles of varying sizes). No chemical stimuli were  
 279 tested on the studied organisms in this work, so their behaviour analysed corresponds to natural response.  
 280 In addition to the tracking accuracy evaluation, the natural locomotive characteristics as described by  
 281 movement velocity, acceleration and direction are also analysed on the video datasets to test the dynamic  
 282 behaviour analysis capability of the proposed system.

### 283 **Small biological organism datasets**

284 Microscopic time-lapse videos of three types of small organism models: zebrafish, *Artemia* and *Daphnia*  
 285 were applied to evaluate the proposed MSBOTS platform. Both low frame rate videos (of 14 or 15 fps  
 286 recorded by a AD7013MT Dino-Lite microscope) and high frame rate videos (captured by an UI-3360CP-  
 287 C-HQ microscope) are tested in this work.

288 Wild zebrafish (*Danio rerio*) embryos were incubated at 28°C in a petri dish filled with an E3 medium.  
 289 Zebrafish larvae were obtained from the hatched embryos five days post-fertilization. Zebrafish larvae  
 290 were transferred to round poly (methyl methacrylate) (PMMA) housing wells for shooting microscopic  
 291 time-lapse videos. The zebrafish dataset consists of 10 video sequences with 3056 frames in total: nine  
 292 zebrafish larvae videos captured as prescribed here and one adult zebrafish video provided by Pérez-  
 293 Escudero et al. (2014) from their publicly available online repository ('Example video of 5 zebrafish' at  
 294 <http://www.idtracker.es/download>). The size of the zebrafish larvae video frames is 960 pixels x 1280  
 295 pixels, and the average zebrafish larvae size is around 1900 pixels. More details about the larvae zebrafish  
 296 dataset and its generation can be found in our previous work (Wang et al., 2017b).

297 Cysts of the marine crustacean *Artemia franciscana* and freshwater *Daphnia magna* were hatched  
 298 and cultured according to the Artoxkit-M and Daphtoxkit-F (MicroBioTests Inc., Belgium) standard  
 299 operating protocols. *Artemia franciscana* were hatched in a petri dish filled with sea water (pH 8.0 ± 0.5)  
 300 at 24 ± 0.5°C under exposure to 3000-4000 lux light source for 30 hours. *Artemia* were placed into a group  
 301 of 10 in a miniaturised Lab-on-a-Chip (LOC) chamber as per Solis et al. (2015) when shooting videos  
 302 with microfluidics infused at a flow rate of 5.25 mL/h. Five *Daphnia magna* neonates were randomly  
 303 selected and transferred into a petri dish with the temperature maintained at 20.0 ± 0.5°C. The *Artemia*  
 304 *franciscana* and *Daphnia magna* dataset consists of 5 video sequences each with 4802 frames and 4804  
 305 frames in total, respectively.

306 *Artemia franciscana* microscopic videos containing 5 organisms and artifacts (bubbles of different  
 307 sizes, video sequences 1-5), with Fig. 4b a microscopic video frame example of *Artemia franciscana*  
 308 in 480 pixels x 640 pixels. The average size of an *Artemia franciscana* object is approximately 500  
 309 pixels. *Daphnia magna* microscopic videos containing 10 organisms and artifacts (bubbles and impurities  
 310 of different sizes, video sequences 1-5), with Fig. 4c a microscopic video frame example of *Daphnia*  
 311 *magna* in 480 pixels x 640 pixels. The average size of *Daphnia magna* tested is approximately 400 pixels.  
 312 Both the *Artemia* and *Daphnia* videos were ordered randomly to test the flexibility and feasibility of the  
 313 proposed system.

#### 314 Tracking evaluation metrics

315 To objectively and quantitatively evaluate the tracking performance of the proposed MSBOTS platform,  
 316 the widely utilised standard metric, Classification of Events, Activities and Relationships (CLEAR MOT)  
 317 (Bernardin and Stiefelhagen, 2008), for Multiple Object Tracking (MOT) is employed in this paper.  
 318 CLEAR MOT comprises two metrics: Multiple Object Tracking Precision (MOTP) as presented by  
 319 Equation (9) and Multiple Object Tracking Accuracy (MOTA) as shown by Equation (10). MOTP  
 320 measures the position precision of all segmented organisms compared to that of the manually labelled  
 321 ground truth in every video frame, whereas MOTA estimates the individual trajectory accuracy (the ability  
 322 to produce exactly one trajectory per organism with a consistent label over time).

$$MOTP = \frac{\sum_{i,t} |P_{i,t} - GT_{i,t}|}{\sum_t N_t} \quad (9)$$

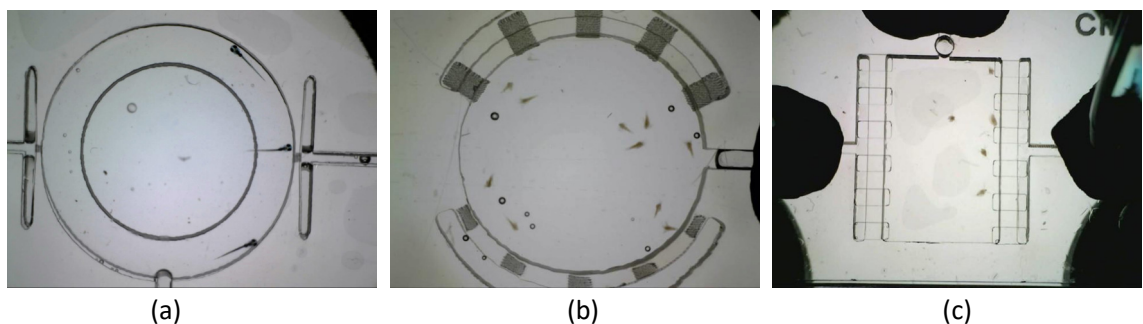


**Figure 4.** Microscopic video frame examples of (a) zebrafish larvae (960 pixels x 1280 pixels), (b) *Artemia franciscana* (480 pixels x 640 pixels), and (c) *Daphnia magna* (480 pixels x 640 pixels). The average sizes of zebrafish larvae, *Artemia* and *Daphnia* tested are approximately 1900, 500 and 400 pixels, respectively.

$$MOTA = 1 - \frac{\sum_t (M_t + FP_t + SII_t)}{\sum_t g_t} \quad (10)$$

where  $|P_{i,t} - GT_{i,t}|$  is the Euclidian distance between the estimated centroid position of the  $i$ -th detected organism  $P_i(t)$  in the frame  $t$ . Its position in the manually labeled ground truth is denoted as  $(GT_{i,t})$  and  $N_t$  indicates the total number of segmented organisms in the ground truth in frame  $t$ . The smaller the MOTP value, the more precise the segmentation result.

MOTP measures the organism segmentation accuracy compared with the ground truth, whereas the MOTA metric emphasises the evaluation of the individual tracking trajectories, where  $M_t$ ,  $FP_t$ , and  $SII_t$  indicate the number of missed detections, false positive detection (i.e., image noise fragments segmented as organisms), and the Swapping of Individual Identities (SII), respectively, in the frame  $t$ . And  $g_t$  means the total number of organisms detected in frame  $t$ . The ideal value of MOTA is 1, and the value decreases with the occurrence of detection errors and identity swapping. Comparing with the total number of detected organisms, the MOTA value will generate negative numbers (as shown in Fig. 5a) when the combination of detection errors and identity swapping is high, which implies low system reliability and the resultant tracking trajectories should be considered as unreliable.

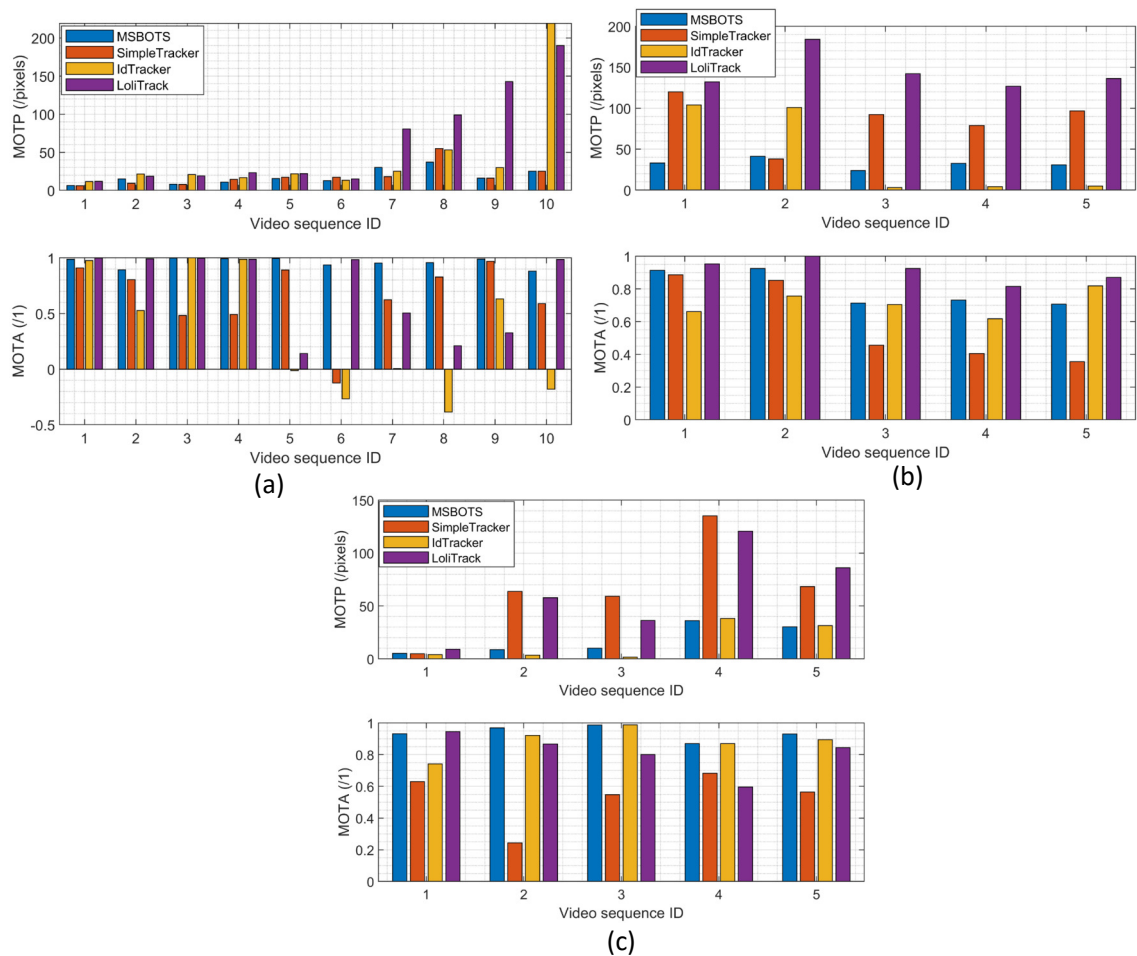


**Figure 5.** Evaluation of tracking results comparing the proposed system MSBOTS to existing systems - SimpleTracker (Bourgeois and Lassalle, 1971), idTracker (Pérez-Escudero et al., 2014) and LoliTrack (Závorka et al., 2017) - using videos of three types of small biological organism. (a), (b) and (c) show the estimated MOTP and MOTA values for zebrafish, *Artemia* and *Daphnia* video datasets, respectively. MOTP values measure the segmentation performance, and the smaller the value the higher the segmentation accuracy. MOTA compares the accuracy of the resultant individual tracking trajectories, with a higher value denoting a more accurate result.

### 336 Tracking accuracy evaluation

337 To evaluate the proposed tracking system, its tracking performance over the microscopic video dataset is  
338 compared with the well-known multiple object tracking platform idTracker (Pérez-Escudero et al., 2014),  
339 SimpleTracker (Bourgeois and Lassalle, 1971) (using the Kuhn-Munkres tracking algorithm for initial  
340 association and the nearest neighbourhood to directly connect trajectory fragments, without considering  
341 missed organisms), and the off-the-shelf commercial LoliTrack system (Závorka et al., 2017). Fig. 5  
342 shows the estimated tracking accuracy measured by the MOTP and MOTA metrics, with Fig. 5a showing  
343 results from zebrafish videos, Fig. 5b showing *Artemia* videos, and Fig. 5c showing *Daphnia* videos.

344 It can be seen from Fig. 5a (the upper MOTP figure) that the positions of detected organisms using  
345 adult and larvae zebrafish videos consistently exhibit the smallest distance differences with the manually  
346 labelled ground truth positions amongst all the methods tested. The proposed MSBOTS approach  
347 resulted in overall smaller MOTP values of 0.92, 25.59, and 44.48 pixels (71.59% increase) compared  
348 to SimpleTracker, idTracker, and LoliTrack, respectively. The improved organism position detection  
349 results demonstrate the accuracy of the theoretical position estimation based on the organism detection  
350 and segmentation results using the adaptive GMM model and post-processing in the proposed MSBOTS  
351 system. Supplementary Table S1 summarises the estimated tracking accuracy measured by MOTP and  
352 MOTA values across all the zebrafish video sequences.

353 All of the methods performed well for the position accuracy of detected organisms when the videos had  
354 a clear background, as shown by sequences 1-6. However, the location errors measured by MOTP for the  
355 detected organisms in the zebrafish videos compared to the ground-truth did not decrease as dramatically  
356 as LoliTrack or idTracker with increasingly complex video backgrounds, as shown by the MOTP values  
357 in sequences 7-10 in Fig. 5a. Accordingly, the proposed MSBOTS method still out-performed the existing  
358 approaches when taking into account mis-detection, false positive segmentation and identity swapping,  
359 with 31.20%, 63.01%, and 24.61% higher MOTA values than SimpleTracker, idTracker, and LoliTrack,  
360 respectively. This was mainly achieved by the ability to estimate the positions of the mis-detected or  
361 overlapped organisms using their neighbour position knowledge from the segmentation results in the  
362 proposed MSBOTS platform. In addition, the bridging of trajectory fragments in MSBOTS based on  
363 the extended Hungarian assignment algorithm (Bourgeois and Lassalle, 1971) when there are multiple  
364 unmatched trajectory fragments decreased the possibility of individual identity swapping, compared with  
365 SimpleTracker, which only used a distance metric by nearest neighbour algorithm (which in turn can  
366 generate identity swapping during the gap bridging process).

367 In addition, Fig. 5b and Fig. 5c show the tracking accuracy evaluation using *Artemia franciscana*  
368 and freshwater *Daphnia magna* videos, respectively, to test the generalisation of the proposed MSBOTS  
369 system on other small organisms with movement characteristics different to zebrafish larvae. *Artemia*  
370 display flexible movement and vary according to surrounding fluidics (Tyson, 1974; Williams, 1994), and  
371 *Daphnia* exhibits short, jerky hopping movement in water (Rottmann et al., 1992)). The overall tracking  
372 accuracy performance of the proposed MSBOTS method is consistent for the tested videos on these two  
373 organism types. The detailed data on tracking accuracy measured by MOTP and MOTA values can be  
374 seen in Supplementary Table S2 & S3.

375 As can be seen from the MOTP values in Fig. 5b, the proposed method exhibits 47.68 pixels smaller  
376 standard deviation than the idTracker system, which illustrated the usability of the proposed system on  
377 *Artemia* microscopic videos and the enhanced ability on *Artemia* detection accuracy. Though idTracker  
378 can produce smaller organism position estimation errors (MOTP) as shown by sequences 3-5 in Fig. 5b,  
379 the mean MOTA value is 7.07%, and 6.44% less than the proposed MSBOTS and LoliTrack, respectively,  
380 which illustrates the existence of a similar detection problem when testing zebrafish larvae. That is, the  
381 organism is detected as background, and impurities as an organism, due to their small size differentiation  
382 and similar movement characteristics when the organism stops moving or the water impurities are stirred  
383 up by organism movement; this further causes identity confusion.

384 Fig. 5c shows the overall tracking accuracy of the proposed MSBOTS system and idTracker consistently  
385 outperformed the other two systems under comparison, measured by MOTP and MOTA. However,  
386 the mean MOTA value of the proposed MSBOTS system is still 5.48% higher than idTracker. The  
387 generalised tracking accuracy of the proposed MSBOTS system is further illustrated by applying it to  
388 *Daphnia* video sequences with short, jerky hopping movement characteristics, compared with these  
389 existing systems.

### 390 Analysis of organism movement characteristics

391 To explore the capability of the proposed MSBOTS approach in analysing organism movement character-  
 392 istics, this paper presents the estimation of movement velocity, acceleration and direction calculated from  
 393 the individual tracking trajectories.

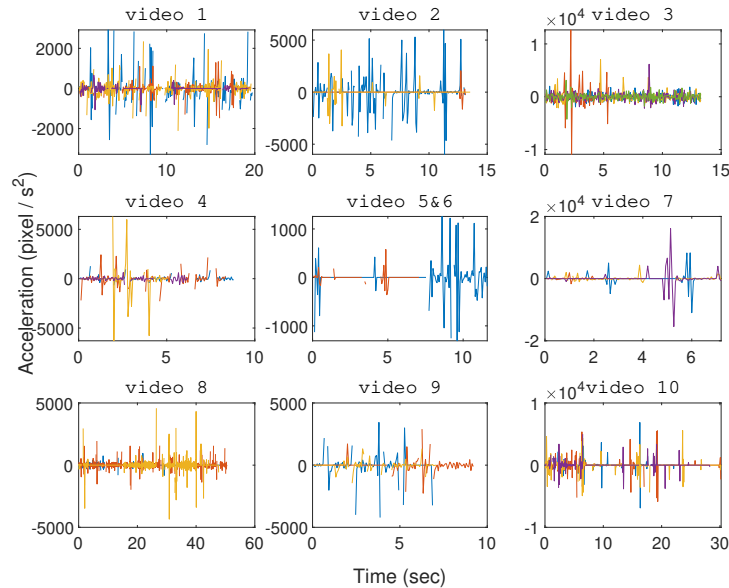


**Figure 6.** Organism movement acceleration over time for every tested zebrafish video ( one video per subplot), with the centre subplot combining the results of videos 5 and 6 housing a single zebrafish larvae each. The line colors represent different zebrafish individuals in every video.

394 Fig. 6 shows the movement acceleration analysis for each zebrafish video using the resultant tracking  
 395 trajectories generated by the proposed MSBOTS. It was found that in Hinz and de Polavieja (2017), the  
 396 interaction and movement of zebrafish larvae was very close to zero by 7 dpf. As shown in Fig. 6, in  
 397 general the variation of movement speed (shown by the computed acceleration values) that is obviously  
 398 visually perceptible to the human eye occurred only within approximately 10 seconds, as tested in the 10  
 399 adult and larvae zebrafish videos. This is due to the natural (anxious) response of zebrafish when turning  
 400 on the imaging camera (Peng et al., 2016)). The zebrafish movement speeds are more subtle from this  
 401 point on, which is consistent with the zebrafish movement characteristics found in Peng et al. (2016);  
 402 Hinz and de Polavieja (2017).

403 As organism movement speed and direction changes can provide insight into the interaction rules  
 404 (Hinz and de Polavieja, 2017), Fig. 7 shows an example of the calculated velocity and movement direction  
 405 results for each zebrafish video, respectively. The equal number of boxes with the number of zebrafish  
 406 housing in each video show that all individuals were successfully assigned with one identity (which  
 407 also illustrated the one-to-one organism mapping accuracy in the proposed MSBOTS system), and the  
 408 median velocity (labelled by the red line inside each box) of each larvae indicates the consistent movement  
 409 characteristic within the same housing well. Mean, minimum and maximum velocity values can also be  
 410 easily obtained from the visual box plot shown in Fig. 7.

411 There is no specific speed requirement for the organisms that can be tracked by the MSBOTS platform.  
 412 Both organisms travelling at high speed or average low speed as illustrated by Fig. 6 and Fig. 7a,  
 413 respectively, can be accurately detected and tracked over time by the system. Thus, this system can be  
 414 used for automatic tracking, comparison and analysis of small organisms in natural response or under the  
 415 exposure of testing chemicals. The recommended lowest frame rate of time-lapse videos is 14 f/s as in the  
 416 tested dataset from trial-and-error comparison.

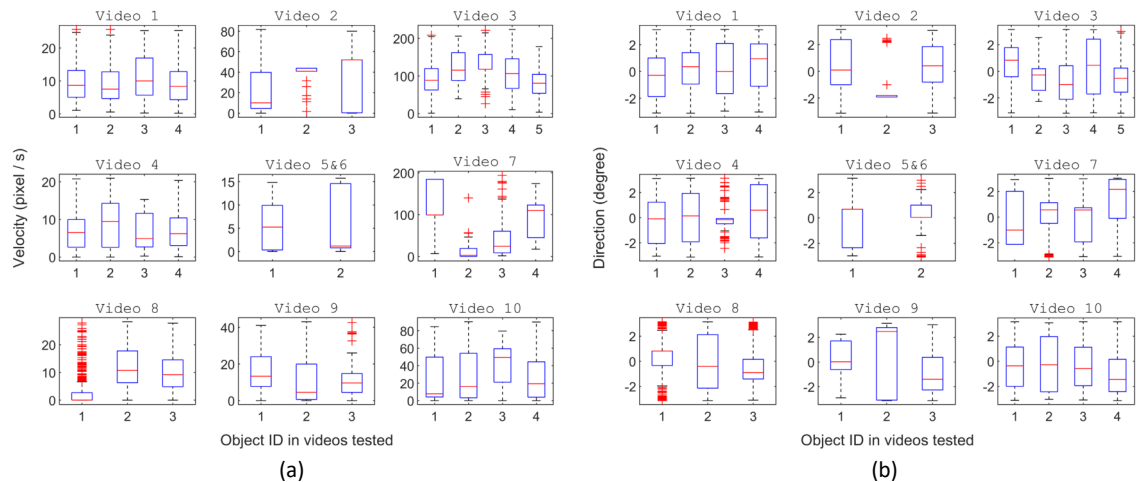


**Figure 7.** Analysis of zebrafish locomotion characteristics across video sequences, where (a) and (b) show movement speed and direction analysis of individual organisms, respectively, in very video frame (the centre subplots combines the results of single zebrafish larvae in videos 5 & 6).

## CONCLUSION

417

418 Accurate automatic tracking for multiple small biological organisms provides an efficient approach for  
 419 many biomedical and ecotoxicity applications. However, organism mis-detection and occlusion are  
 420 inevitable problems when detecting and segmenting these small biological organisms from time-lapse  
 421 microscopic videos. The detection and segmentation becomes more challenging when tracking small  
 422 biological aquatic organisms compared with general objects, which in turn affects the subsequent organism  
 423 tracking processes. To improve the tracking accuracy based on the non-ideal organism detection and  
 424 segmentation results, extending on and improving our previous work, this paper presents a Multiple Small  
 425 Biological Organism Tracking System (MSBOTS), combining a multiple object association algorithm  
 426 for linking detected objects frame-by-frame and tracking trajectory adjustment techniques. To address  
 427 segmentation errors due to mis-detected or occluded organisms, the proposed MSBOTS approach es-  
 428 timated positions of organisms in interim frames using corresponding points in neighbouring frames.  
 429 Finally, the calculated points are applied to connect and adjust the tracking trajectory fragments from  
 430 the initial association based on an extended Kuhn-Munkres algorithm. The proposed system was tested  
 431 on three different types of small organisms with variant movement characteristics, using 20 videos in  
 432 total for evaluation. The resulted tracking accuracy of the proposed system outperformed three existing  
 433 (state-of-the-art or commercial) tracking systems. Moreover, this system also provides locomotive char-  
 434 acteristic analysis using the generated individual tracking trajectories to facilitate small organism behaviour  
 435 analysis research. Behavioural rules and new medicine or chemical effects on the dynamic behaviour of  
 436 organisms can thus be investigated using the proposed behaviour analysis module, enabling an automatic  
 437 and quantitative movement analysis to the related experiments.

## DATA AVAILABILITY STATEMENTS

438

439 The datasets analysed during the current study were made fully publicly available in the online repository,  
 440 <https://github.com/Xiao-ying> and <https://github.com/Xiao-ying/moving-zebrafish-larvae-segmentation-and-tracking-dataset/tree/master/Data>. The analysed adult zebrafish video was downloaded from the  
 441 publicly available online repository <http://www.idtracker.es/download> (the 'Example video of 5 zebrafish').  
 442 The developed MSBOTS system and the software to analyse locomotive characteristics of individual  
 443 organisms can also be downloaded from the same repository.  
 444

## REFERENCES

445

446 Alyuruk, H., Demir, G. K., and Cavas, L. (2013). A video tracking based improvement of acute toxicity  
 447 test on artemia salina. *Marine and Freshwater Behaviour and Physiology*, 46(4):251–266.

- 448 Bernardin, K. and Stiefelwagen, R. (2008). Evaluating multiple object tracking performance: the clear  
449 mot metrics. *EURASIP Journal on Image and Video Processing*, pages 1687–5281.
- 450 Bourgeois, F. and Lassalle, J. C. (1971). An extension of the munkres algorithm for the assignment  
451 problem to rectangular matrices. *Communications of the ACM*, 14(12):802–804.
- 452 Colwill, R. M. and Creton, R. (2011). Locomotor behaviors in zebrafish (*danio rerio*) larvae. *Behavioural*  
453 *Processes*, 86(2):222–229.
- 454 Comeche, A., Martín-Villamil, M., Picó, Y., and Varó, I. (2017). Effect of methylparaben in artemia  
455 franciscana. *Comparative Biochemistry and Physiology Part C: Toxicology & Pharmacology*, 199:98–  
456 105.
- 457 Conklin, E. E., Lee, K. L., Schlabach, S. A., and Woods, I. G. (2015). Videohacking: automated tracking  
458 and quantification of locomotor behavior with open source software and off-the-shelf video equipment.  
459 *Journal of Undergraduate Neuroscience Education*, 13(3):A120–A125.
- 460 Dur, G., Souissi, S., Schmitt, F., G., M. F., S., M. M., and S., H. J. (2011). Effects of animal density,  
461 volume, and the use of 2d/3d recording on behavioral studies of copepods. *Hydrobiologia*, 666(1):197–  
462 214.
- 463 Ekvall, M. T., Bianco, G., Linse, S., Linke, H., Backman, J., and Hansson, L. A. (2013). Three-dimensional  
464 tracking of small aquatic organisms using fluorescent nanoparticles. *PloS One*, 8(11):e78498.
- 465 Günel, S., Rhodin, H., Morales, D., J., C., P., P. R., and P., F. (2019). Deepfly3d, a deep learning-based  
466 approach for 3d limb and appendage tracking in tethered, adult drosophila. *eLife*, 8.
- 467 Habibi, Y., Sulistyaningrum, D. R., and Setiyono, B. (2017). A new algorithm for small object tracking  
468 based on super-resolution technique. In *AIP Conference Proceedings*, volume 1867, pages 20–24. AIP  
469 Publishing.
- 470 Harold, W. K. (1955). The hungarian method for the assignment problem. *Naval Research Logistics*  
471 *Quarterly*, 2:83–97.
- 472 Hinz, R. C. and de Polavieja, G. G. (2017). Ontogeny of collective behavior reveals a simple attraction  
473 rule. *Proceedings of the National Academy of Sciences*, 114(9):2295–2300.
- 474 James, D. M., Kozol, R. A., Kajiwar, Y. J., L., W. A., C., S. E., D., B. J., M., K., B., B. M., and E., D. J.  
475 (2019). Intestinal dysmotility in a zebrafish (*danio rerio*) shank3a; shank3b mutant model of autism.  
476 *Molecular Autism*, 10(1):3–18.
- 477 Lard, M., Backman, J., Yakovleva, M., Danielsson, B., and Hansson, L. A. (2010). Tracking the small  
478 with the smallest-using nanotechnology in tracking zooplankton. *PloS One*, 5(10):e13516.
- 479 Liu, Y. W., Ma, P., Cassidy, P. A., Carmer, R., Zhang, G. N., Venkatraman, P., Brown, S. A., Pang, C. P.,  
480 Zhong, W. X., Zhang, M. Z., and F., L. Y. (2017). Statistical analysis of zebrafish locomotor behaviour  
481 by generalized linear mixed models. *Scientific Reports*, 7.
- 482 Mallick, M., Vo, B. N., Kirubarajan, T., and Arulampalam, S. (2013). Introduction to the issue on  
483 multitarget tracking. *IEEE Journal of Selected Topics in Signal Processing*, 7(3):373–375.
- 484 Marechal, J. P., Hellio, C., Sebire, M., and Clare, A. (2004). Settlement behaviour of marine invertebrate  
485 larvae measured by ethovision 3.0. *Biofouling*, 20(4-5):211–217.
- 486 Martineau, P. R. and Mourrain, P. (2013). Tracking zebrafish larvae in group—status and perspectives.  
487 *Methods (San Diego, Calif.)*, 62(3):292—303.
- 488 Munkres, J. (1957). Algorithms for the assignment and transportation problems. *Journal of the society*  
489 *for industrial and applied mathematics*, 5(1):32–38.
- 490 Nema, S., Hasan, W., Bhargava, A., and Bhargava, Y. (2016). A novel method for automated tracking  
491 and quantification of adult zebrafish behaviour during anxiety. *Journal of Neuroscience Methods*,  
492 271:65–75.
- 493 Noss, C., Lorke, A., and Niehaus, E. (2013). Three-dimensional tracking of multiple aquatic organisms  
494 with a two camera system. *Limnology and Oceanography: Methods*, 11(3):139–150.
- 495 Peng, X. L., Lin, J., Zhu, Y. D., Liu, X. Y., Zhang, Y. L., Ji, Y. X., Y., Z., N., G., and Q., L. (2016). Anxiety-  
496 related behavioral responses of pentylenetetrazole-treated zebrafish larvae to light-dark transitions.  
497 *Pharmacology Biochemistry and Behavior*, 145:55–65.
- 498 Pérez-Escudero, A., Vicente-Page, J., Hinz, R. C., Arganda, S., and De Polavieja, G. G. (2014). idtracker:  
499 tracking individuals in a group by automatic identification of unmarked animals. *Nature Methods*,  
500 11(7):743–748.
- 501 Poynton, H. C., Varshavsky, J. R., Chang, B., G., C., S., C., S., H. P., V., L. A., J., B. D., K., K., C., T. E.,  
502 E.J., P., O., H., and D., V. C. (2007). *Daphnia magna* ecotoxicogenomics provides mechanistic insights

- 503 into metal toxicity. *Environmental Science & Technology*, 41(3):1044–1050.
- 504 Rashid, M. T., Frasca, M., Ali, A. A., Ali, R. S., L., F., and G., X. M. (2012). Artemia swarm dynamics  
505 and path tracking. *Nonlinear Dynamics*, 68(4):555–563.
- 506 Rottmann, R. W., Graves, J. S., Watson, C., and Yanong, R. E. (1992). *Culture Techniques of Moina: The  
507 ideal Daphnia for feeding freshwater fish fry*. Florida Cooperative Extension Service, Institute of Food  
508 and Agricultural Sciences, University of Florida.
- 509 Solis, J., Huang, Y. S., Wlodkovic, D., and Reyes, C. (2015). Microfluidic environment and tracking  
510 analysis for the observation of artemia franciscana. *Proceedings of sthe 26th British Machine Vision  
511 Conference*.
- 512 Tyson, G. E. (1974). Ultrastructure of a spirochete found in tissues of the brine shrimp, artemia salina.  
513 *Archives of Microbiology*, 99(1):281–294.
- 514 Usami, M. (2004). An ultra-small rfid chip:/spl mu/-chip. In *Advanced System Integrated Circuits.  
515 Proceedings of 2004 IEEE Asia-Pacific Conference on*, pages 2–5. IEEE.
- 516 Wang, X. (2018). *computer vision techniques applied to automatic biological organism segmentation and  
517 tracking*. PhD thesis, School of Engineering.
- 518 Wang, X. Y., Cheng, E., Burnett, I. S., Huang, Y. S., and Wlodkovic, D. (2017a). Automatic multiple  
519 zebrafish larvae tracking in unconstrained microscopic video conditions. *Scientific Reports*, 7(1):1–8.
- 520 Wang, X. Y., Cheng, E., Burnett, I. S., S., H. Y., and D., W. (2017b). Crowdsourced generation of  
521 annotated video datasets: a zebrafish larvae dataset for video segmentation and tracking evaluation. In  
522 *2017 IEEE Life Sciences Conference (LSC)*, pages 274–277. IEEE.
- 523 Wang, X. Y., Cheng, E., Burnett, I. S., Wilkinson, R., and Lech, M. (2018). Automatic tracking of  
524 multiple zebrafish larvae with resilience against segmentation errors. In *2018 IEEE 15th International  
525 Symposium on Biomedical Imaging (ISBI 2018)*, pages 1157–1160. IEEE.
- 526 Williams, T. A. (1994). A model of rowing propulsion and the ontogeny of locomotion in artemia larvae.  
527 *The Biological Bulletin*, 187(2):164–173.
- 528 Zhiping, X. and Cheng, X. E. (2017). Zebrafish tracking using convolutional neural networks. *Scientific  
529 Reports*, 7.
- 530 Zhou, Y. Z., Cattley, R. T., Cario, C. L., Bai, Q., and Burton, E. A. (2014). Quantification of larval  
531 zebrafish motor function in multi-well plates using open-source matlab® applications. *Nature Protocols*,  
532 9(7):1533–1548.
- 533 Zivkovic, Z. and Heijden, V. D. F. (2006). Efficient adaptive density estimation per image pixel for the  
534 task of background subtraction. *Pattern Recognition Letters*, 27(7):773–780.
- 535 Zivkovic, Z. and Van Der Heijden, F. (2004). Recursive unsupervised learning of finite mixture models.  
536 *IEEE Transactions on Pattern Analysis and Machine Intelligence*, 26(5):651–656.
- 537 Závorka, L., Koeck, B., Cucherousset, J., Brijs, J., Näslund, J., Aldvén, D., Höjesjö, J., Fleming, I. A.,  
538 and Johnsson, J. I. (2017). Co-existence with non-native brook trout breaks down the integration of  
539 phenotypic traits in brown trout parr. *Functional Ecology*, 31(8):1582–1591.